Through-Bond Orbital Coupling in End-Functionalized Bicyclohexylidenes − Photoelectron Spectroscopy and Ab initio SCF−MO Calculations

Albert W. Marsman,[a] Remco W. A. Havenith,[a,b] Sabine Bethke,[c] Leonardus W. Jenneskens,*[a] Rolf Gleiter,[c] and Joop H. van Lenthe[b]

Keywords: Ab initio calculations / Oligo(cyclohexylidenes) / Photoelectron spectroscopy / Through-bond interactions / Through-space interactions

To establish whether through-bond (TB) orbital interactions occur between the functional groups and the hydrocarbon skeleton in a series of end-functionalized oligo(cyclohexylidenes) **1**–**12**, their He^I photoelectron (PE) spectra were measured and analyzed. Vertical ionization energies, I_{vj}, of the highest occupied molecular orbitals (MOs) of **1**–**12** were assigned using ab initio RHF/6–31G* MO energies ($-\varepsilon_j$) in combination with Koopmans' theorem. Excellent to good agreement was found between the PES and RHF/6–31G* results. In addition, the I_{vj} assignments were further corroborated by a comparison of the PES data of **1**–**12** with those previously reported for appropriate reference compounds **13**–**20**. To assess contributions from through-bond (TB) and/or through-space (TS) interactions, RHF/6–31G*/NBO analyses were performed. The results show that in the cases of **1**–**12**, TS interactions do not occur. TB interactions were unequivocally identified for **1**–**4**, **8**, **10** and **11**–**12**. These TB interactions were found to be relayed via the H_{ax}–C–C–H_{ax} precanonical σ-MOs (σ-PCMOs) of the cyclohexyl-like moieties.

Introduction

Oligo(cyclohexylidenes) consist of cyclohexyl-type rings interconnected by olefinic bonds; the first three representatives of the parent series are 1,1′-bicyclohexylidene (**15**), 1,1′:4′,1′′-tercyclohexylidene (**16**) and 1,1′:4′,1′′:4′′,1′′′-quatercyclohexylidene (**4**) (Figures 1 and 2). Besides a length increment of ca. 4 Å, they possess an alternating σ−π orbital topology. We have shown that end-functionalized derivatives represent semi-rigid, rod-like molecular building blocks, which can be used in the assembly of supramolecular systems.[1]

As a consequence of the σ-π orbital topology of their hydrocarbon skeletons, the oligo(cyclohexylidenes) are capable of relaying electronic interactions *via* a through-bond (TB) orbital interaction mechanism. He^I photoelectron spectroscopy (PES) and ab initio RHF/6−31G* calculations have shown that the two π(C=C) units of **16** do indeed couple (ΔI_{vj} 0.46 eV and $\Delta-\varepsilon_j$ 0.56 eV).[2] The splitting was found to be independent of the possible *syn* or *anti* orientation of the interconnected chair-like, cyclohexyl-type rings of the oligo(cyclohexylidene) framework (Figure 3).

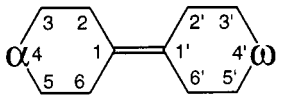

Compound	α	ω
1	H_2C=C	CH_2
2	H_2C=C	C=CH_2
3	$(H_3C)_2C$=C	CH_2
4	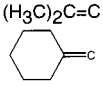	
5	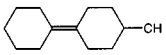	CH_2
6	O=C	CH_2
7	O=C	C=O
8	O=C	S
9	HON=C	CH_2
10	HON=C	S
11	$(NC)_2C$=N	CH_2
12	$(NC)_2C$=N	S

Figure 1. End-functionalized oligo(cyclohexylidenes) **1**−**12**.

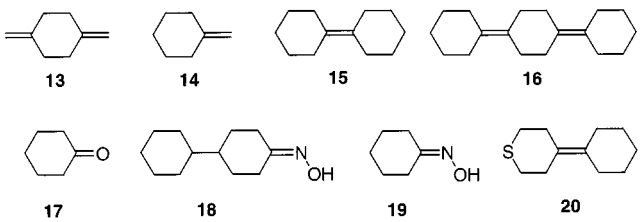

Figure 2. Reference compounds **13**−**20**.

[a] Debye Institute, Department of Physical Organic Chemistry, Utrecht University,
Padualaan 8, 3584 CH Utrecht, The Netherlands
Fax: (internat.) + 31-30/253-4533,
E-mail: jennesk@chem.uu.nl
[b] Debye Institute, Theoretical Chemistry Group, Utrecht University,
Padualaan 8 3584 CH Utrecht, The Netherlands
[c] Organisch-Chemisches Institut der Universität Heidelberg,
Im Neuenheimer Feld 270, 69120 Heidelberg, Germany

  1434−193X/00/0714−2629 $ 17.50+.50/0

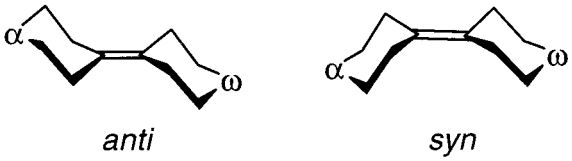

Figure 3. Schematic representation of *anti* and *syn* conformers in oligo(cyclohexylidenes).

RHF/6−31G* Natural Bond Orbital (NBO) analyses revealed that the TB interactions are relayed by (delocalized) precanonical molecular orbitals (PCMOs) encompassing the $H_{ax}-C-C-H_{ax}$ units of the cyclohexyl-type rings.[3−6] The TB mechanism is similar to that reported for interactions between nonconjugated π-units coupled via three intervening σ-type carbon−carbon bonds.[7−9] Hence, if interactions between functional groups incorporated at the α- and/or ω-termini are to be efficiently relayed by an oligo(cyclohexylidene) hydrocarbon skeleton, all interacting orbitals must possess similar energies and belong to the same irreducible representation. Previously, it was shown that these prerequisites are fulfilled by a 3p-sulfur lone pair [Lp_π(S)], namely in oligo(cyclohexylidenes) end-capped with tetrahydro-*4H*-thiopyran.[2] The Lp_π(S) lone pairs couple strongly with the $H_{ax}-C-C-H_{ax}$ units of the cyclohexyl-type rings. In the bis-functionalized sulfur derivatives, a splitting of both Lp_π(S) levels (ca. 0.40 eV) is observed;[2] these interactions are efficiently relayed over a distance of ca. 11.8 Å.

This paper explores the occurrence of TB orbital coupling in oligo(cyclohexylidenes) **1−12**, with different functionalities at their α- and/or ω-termini. Such functionalities include methylidenes [π(C=C)], ketones [π(C=O)], oximes [π(C=N−O)] and dicyanoethylenes [π(C=C(CN$_2$))], in the presence or absence of an additional sulfur atom at the other end-position (Figure 1). Although all functional groups possess π-type orbitals with the proper symmetry for TB interactions with the π(C=C) and the $H_{ax}-C-C-H_{ax}$ units, their energy levels vary considerably. This enables the assessment of energy matching in combination with the effect of an additional perturbation by the Lp_π(S) towards TB orbital coupling. Vertical ionization energies, I_{vj}, of the highest occupied MOs of **1−12** were measured using He^I PES. The PES results are interpreted by band correlations using the reference compounds **13−20** (Figure 2) and RHF/6−31G* calculations, i.e. the energies (ε_j) of the (delocalized) canonical molecular orbitals (CMOs) are compared with the I_{vj} values obtained when applying Koopmans' theorem ($I_{vj} = -\varepsilon_j$).[10] In addition, RHF/6−31G* NBO analyses were carried out to distinguish between through-space (TS) and through-bond (TB) contributions in the cases of **2** and **6−12**.[11−13]

Results and Discussion

Synthesis

4-Methylidene-1,1′-bicyclohexylidene (**1**) and 4,4′-dimethylidene-1,1′-bicyclohexylidene (**2**) were prepared from 1,1′-bicyclohexyliden-4-one (**6**)[1a] and 1,1′-bicyclohexylidene-4,4′-dione (**7**),[1d] respectively, by employing a standard Wittig reaction.[14] 4-Isopropylidene-1,1′-bicyclohexylidene (**3**) was obtained from **6** by using a reported decarboxylative dehydration method.[1] Compounds **4−11** and **18** were prepared as previously reported.[1,15−17] Compound **12** was obtained from **8**[1d] following the Knoevenagel reaction procedure used for the synthesis of **11**a.

Ground-State Conformational Properties of Oligo(cyclohexylidenes)

Two interconnected chair-like, cyclohexyl-type rings in oligo(cyclohexylidenes) can adopt an *anti* or *syn* orientation with respect to each other (Figure 3). Whereas single-crystal X-ray structural analyses suggest that, in the solid state, oligo(cyclohexylidene) hydrocarbon skeletons predominantly prefer an *anti* conformation, a staircase-like geometry in other words,[1,2,18] they are conformationally mobile in solution (^{1}H NMR).[1] Ab initio RHF/6−31G* calculations for *anti*- and *syn*-1,1′-bicyclohexylidene (**15**, Figure 2) indicated that both conformers possess nearly identical total energies; i.e. a ca. 1:1 equilibrium mixture is expected both in the gas phase and in solution. Consequently, the gas phase PE spectra **1−12** are expected to originate from mixtures of conformers.[2] In the cases of **15** and **16** and their analogues containing sulfur atoms at the α- and/or ω- termini, RHF/6−31G* calculations have shown that both the ε_j values and the character of the highest occupied MOs are independent of conformational differences due to *anti* and *syn* isomerism.[2,19]

For ketones **6** and **7**, however, the cyclohexyl-type rings bearing the ketone group can adopt *twist-boat* conformations both in the solid state and in solution [cf. also *twist-boat* 1,4-cyclohexanedione (D_2)].[20] In this respect, the reported single-crystal X-ray structure of **7** is of interest. In the unit cell, two crystallographically independent molecules are found.[1d] Whereas one possesses an *anti* (C_{2h}) conformation (chair-like, cyclohexyl-type rings), the other has two twist-boat (C_i), cyclohexyl-type rings. RHF/6−31G* calculations on the *anti* and the *twist-boat* conformers of **7** revealed that, although the $-\varepsilon_j$ values of the MOs of primarily π(C=C) character differ ($\Delta-\varepsilon_j$ 0.24 eV), the $-\varepsilon_j$ values of their oxygen lone pairs Lp_n(O) are similar ($\Delta-\varepsilon_j$ 0.02 eV; Table 3). This suggests that, for the interpretation of the PES results, only the *anti* conformers have to be taken into account. Hence, the *anti* conformers of the oligo(cyclohexylidenes) **1−12** (Figure 1) and of **18** (Figure 2) were studied at the RHF/6−31G* level of theory (C_s; **1**, **3**, **6**, **8**, **11** and **12**, C_{2h}; **2**, **4**, **5** and **7** and C_1; **9**, **10** and **18**). The RHF/6−31G* geometries of *anti*-**15**,[2,18] *anti*/*anti*-**16**,[2,21,22] *anti*-**9**[1d] and *anti*-**18**[1c,15,17] are in satisfactory agreement with available single-crystal X-ray structural data. Salient structural features of **9** and **18** are presented in Table 1.

Photoelectron Spectra of 1−5

It is well documented that the He^I PE spectrum of 1,4-dimethylidenecyclohexane (**13**) exhibits two split π(C=CH$_2$)

Table 1. Salient structural features of the single-crystal X-ray and RHF/6−31G* structures of *anti*-**9** (see ref.[1c]) and its saturated analogue *anti*-**18** (see ref.[1d]). For atom numbering see Figure 1

Bond lengths [Å]	X-ray	6−31G*	Valence angles [°]	X-ray	6−31G*
anti−**9**[a]					
C1−C1′	1.338(3)/1.334(4)	1.332	N−C4−C3	121.5(3)/120.2(3)	126.8
C4−N	1.277(3)/1.278(3)	1.256	N−C4−C5	119.5(3)/123.2(3)	117.2
N−O	1.487(5)/1.468(4)	1.379	C3−C4−C5	118.8(2)/116.5(2)	115.9
C4−C5[b]	1.497(4)/1.485(4)	1.506	C4−N−O[c]	114.2(3)/113.5(3)	113.6
C4−C3	1.496(4)/1.496(4)	1.507	C4−N−O[c]	114.0(3)/115.3(3)	113.6
anti−**18**					
C1−C1′	1.539(3)	1.550	N−C4−C3	123.0(2)	127.2
C4−N	1.269(4)	1.256	N−C4−C5	121.2(2)	117.7
N−O	1.466(4)	1.380	C3−C4−C5	115.8(2)	115.1
C4−C5[b]	1.492(4)	1.504	C4−N−O[c]	114.3(2)	113.5
C4−C3	1.491(3)	1.505	C4−N−O[c]	114.3(3)	113.5

[a] Compound **9** has two crystallographically independent molecules in the unit cell, which both have the *anti* conformation, but differ slightly with respect to their structural parameters (ref.[1c,1d]). − [b] C4−C5 is positioned *anti* with respect to the oxime group. − [c] The oxime groups is disordered over two positions with respect to the C=N bond.

bands positioned at 9.0 and 9.5 eV (ΔI_{vj} 0.5 eV).[11] This splitting is reproduced by RHF/6−31G calculations ($\Delta-\varepsilon_j$ 0.69 eV).[21] NBO analyses revealed that TB interactions involving σ orbitals of the $H_{ax}-C-C-H_{ax}$ units of the cyclohexyl-type rings occur.[9] To assess whether similar interactions take place between two π(C=CH_2) moieties separated by a 1,1′-bicyclohexylidene moiety, the He^I PE spectra of **1** and **2** were measured (Figure 4). The vertical ionization energies, I_{vj}, of the bands situated below ca. 10 eV are listed in Table 2. The PE spectrum of **1** contains two bands with vibrational progressions at 8.25 eV ($\tilde{\nu} \approx 1371\ cm^{-1}$) and 9.11 eV ($\tilde{\nu} \approx 1613\ cm^{-1}$). Correlation with PES data from methylidenecyclohexane (**14**, 9.08 eV)[11] and 1,1′-bicyclohexylidene (**15**, 8.16 eV)[2] suggests an assignment of the 8.25 eV and 9.11 eV bands of **1** to ionization at the central π(C=C) and the terminal π(C=CH_2) orbitals, respectively (Figure 5). In analogy, the 8.26 eV band of **2** is attributed to an ionization at the central π(C=C) orbital (Figure 5). The next two bands of **2**, at 8.96 eV and 9.26 eV, are assigned to ionizations at the two linear combinations of the terminal π(C=CH_2) units [$a_g(\pi^+)$ and $b_u(\pi^-)$], i.e. they are split by 0.3 eV. Although the π(C=CH_2) band of **1** has a vibrational progression ($\tilde{\nu} \approx 1617\ cm^{-1}$) that corresponds to the ν(C=CH_2) stretch vibration of its radical cation,[23,24] the separation between bands 2 and 3 in the PE spectrum of **2** is larger ($\tilde{\nu} \approx$ 2420 cm^{-1}, Figure 4). Hence, this suggests the occurrence of orbital coupling and band splitting. This is supported by the observation that a similar center of gravity is found for the split π(C=CH_2) bands for **2** and **13** (**2**, 9.11 eV and **13**,[11] 9.25 eV). The RHF/6−31G* MO sequence and splitting are in line with the experimental results (Table 2). The splitting of the terminal π(C=CH_2) units of **2** (ΔI_{vj} 0.3 eV and $\Delta-\varepsilon_j$ 0.22 eV) is smaller than that found for **13** (ΔI_{vj} 0.5 eV and $\Delta-\varepsilon_j$ 0.69 eV[11,21]). Since comparable splittings are found for **13** and **16** (ΔI_{vj} 0.46 eV and $\Delta-\varepsilon_j$ 0.56 eV),[2,21] it appears that the interaction of either the central π(C=C) or the terminal π(C=CH_2) units with the $H_{ax}-C-C-H_{ax}$ σ-orbitals is equally efficient in the case of **2**.

Consequently, the smaller splitting in **2** must originate from inefficient mixing of the π(C=C) and the two π(C=CH_2) orbitals. This can be attributed to their energy separation (ca. 1 eV). A similar conclusion was recently reported for distella-2,2′,6,6′-triene.[9] For this compound, improved orbital mixing and enhanced splitting ($\Delta\Delta I_{vj}$ 0.1 eV[9]) could be achieved by replacing the methylidene [π(C=CH_2)] groups by isopropylidene units [π(C=C(CH_3)$_2$)].[11] Hence, an enhanced interaction would be expected for 4-isopropylidene-1,1′-bicyclohexylidene (**3**, Figure 1) on going from **1** to **3**. Indeed, the energy difference between the central π(C=C) and terminal [π(C=C(CH_3)$_2$)] orbitals decreases due to destabilization of the latter orbital in **3** (Figure 4 and Table 2). The PE spectrum of **3** shows two bands at 7.97 eV and 8.40 eV, with a center of gravity (8.19 eV) that corresponds with the π(C=C) ionization of **15** (8.16 eV[2]). For **3**, the substantial splitting of its π(C=C) orbitals (ΔI_{vj} 0.43 eV, $\Delta-\varepsilon_j$ 0.58 eV) closely resembles that found in the PE spectrum of the structurally related **16** (ΔI_{vj} 0.46 eV, $\Delta-\varepsilon_j$ 0.56 eV).[2]

A similar result is expected for 1,1′:4′,1′′:4′′,1′′′-quatercyclohexylidene (**4**), relative to **2**. In the PE spectrum of **4**, a broad π-MO band (range 7.7−8.7 eV) is observed (Figures 4 and 5 and Table 2). Despite the presence of three distinct maxima (7.9 eV, 8.1 eV and 8.3 eV), straightforward interpretation is hampered by band overlap. Although the presence of vibrational progressions cannot be ruled out, its bandwidth (ca. 1 eV) is in line with the calculated splitting between the three π(C=C) orbitals ($\Delta-\varepsilon_j$ 0.40 and 0.41 eV, Table 2). Since the I_{vj} and $-\varepsilon_j$ values of **1**, **2** and **15**,[2] respectively, differ by ca. −0.4 eV from the orbital of primarily π(C=C) character, the π(C=C) bands of **4** are expected to be positioned at ≈7.8 eV, ≈8.3 eV and ≈8.7 eV (Figures 4 and 5 and Table 2). The occurrence of a splitting is further corroborated by comparison of the PE spectrum of **4** with that of 4,4′-bis(cyclohexylidene-1,1′-bicyclohexyl) (**5**; not shown), which lacks the central π(C=C) bond and, thus, contains two decoupled π(C=C) units. In going from

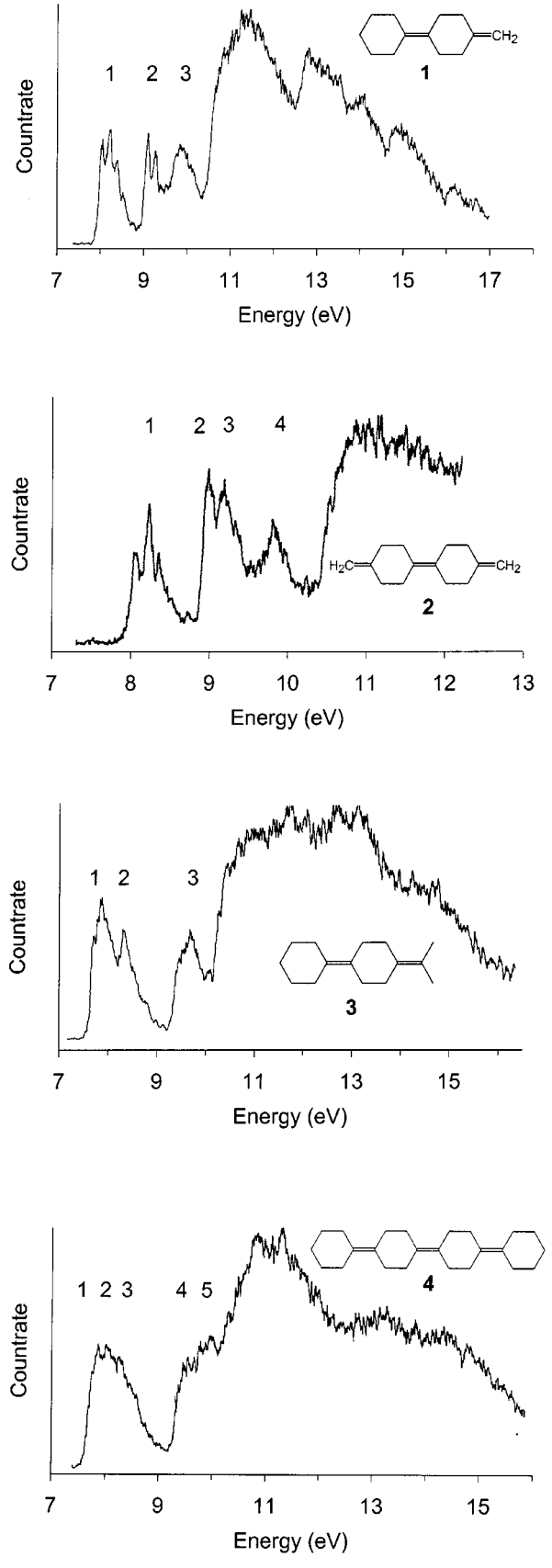

Figure 4. He^{I} Photoelectron spectra of **1**−**4**.

4 to **5**, the width and position of the π(C=C) band of **4** both reduces and shifts to the values for the π(C=C) band of **15** (8.16 eV; bandwidth 0.35 eV).[2,25]

Photoelectron Spectra of 6−8

The He^{I} PE spectra of ketones **6**−**8** are shown in Figure 6 and the I_{vj} values below ca. 10 eV are listed in Table 3. Correlation of the bands of **6** and **7** with those of **15** (8.16 eV[2]) and cyclohexanone (**17**, 9.29 eV, Figure 7)[26] suggests that the first and second bands must be assigned to ionizations at orbitals involving the π(C=C) unit and oxygen lone pairs [Lp_n(O)], respectively. This interpretation is corroborated by the intensities of their PES bands. In going from **15** to **6** to **7**, there is an inductive shift (ca. 0.4 eV) of the π- and σ-type bands to higher energy for each additional C=O moiety. Although the Lp_n(O) band of **7** is broader (ca. 0.14 eV) than that of **6**, no splitting is discernible; i.e. coupling between the Lp_n(O)s of **7** is small. This is supported by the RHF/6−31G* results ($\Delta-\varepsilon_j$ 0.19 eV, Table 3). A similar splitting (ΔI_{vj} ca. 0.15 eV) was found for *twist-boat* 1,4-cyclohexanedione **7** (D_2).[27,28] RHF/6−31G* calculations on *anti*-**7** ($C_{2\,h}$) and *twist-boat*-**7** (C_i), gave identical Lp_n(O) splittings (vide supra, Table 3). The nearly identical Lp_n(O) band positions of **6**, **7** and **17** indicate that the 9.2 eV band of **8** must also be assigned to an Lp_n(O) ionization (Figures 6 and 7). Correlation of the PES bands of **8** at 8.37 eV and 8.94 eV with PES results for **20** [a′ π/Lp_π(S) 8.16 eV and a′ Lp_π(S)/π 8.63 eV, Figure 2],[2] reveals that these bands can be attributed to ionizations at the two linear combinations of the π(C=C) and Lp_π(S) orbitals, taking into account an inductive shift of ca. 0.4 eV due to the C=O moiety. The band separation (ΔI_{vj} 0.57 eV and $\Delta-\varepsilon_j$ 0.56 eV) is in line with that found for **20** (ΔI_{vj} 0.47 eV and $\Delta-\varepsilon_j$ 0.53 eV).

The Lp_n(O) bands of **6**−**8** are broad and of Gaussian-like shape. In general, ionization at nonbonding or weakly bonding orbitals, shows sharp, Franck−Condon-allowed 0←0 transitions [cf. formaldehyde; Lp_n(O) 10.88 eV.[29]] Hence, the observed broadening, also found previously for other diketones, suggests the admixture of cyclohexyl-type σ-orbitals.[27] In the cases of **6**−**8**, these σ-orbitals do not belong to the same irreducible representation as the π(C=C) or highest linear combination of $H_{ax}-C-C-H_{ax}$ orbitals. Hence, the Lp_n(O)s do not couple with the latter orbitals (see also NBO analyses below).

In passing, it is noteworthy that a good agreement is found between the PES results and the RHF/6−31G* data obtained using Koopmans' theorem for the ketones **6**−**8**; in particular the identification and assignment of the Lp_n(O) bands. Hence, the defects of Koopmans' theorem, i.e. deviations from $-\varepsilon_j$ values, do not have to be taken into account.[9]

Photoelectron Spectra of 9−12 and 18

The He^{I} PE spectra of the oximes **9**, **10** and **18** are depicted in Figure 8 (see also Table 4). In the spectrum of **9**, besides a well resolved band at 8.33 eV, three partially re-

Table 2. Vertical ionization energies I_{vj} [eV] and RHF/6−31G* orbital energies $-\varepsilon_j$ [eV] and assignments of *anti*-**1**, *anti*-**2**, *anti*-**3**, *anti*/*anti*/*anti*-**4**, and *anti*/*anti*/*anti*-**5**

Compound[a]	Band (j)	I_{vj}	$-\varepsilon_j$	Assignment[b]
1	1	8.25[c]	8.61	30a′ π(C=C)
(C_s)	2	9.11[d]	9.46	29a′ π(C=CH_2)
	3	9.9	11.13	19a′ σ
2	1	8.26	8.64	$16b_u$ π(C=C)
(C_{2h})	2	8.96	9.40	$16a_g$ π(C=CH_2)/π(C=CH_2)
	3	9.26	9.62	$15b_u$ π(C=CH_2)/π(C=CH_2)
	4	9.90	11.18	$10b_g$ σ
3	1	7.97	8.39	34a′ π(C=C)/π(C=C(CH_3)$_2$)
(C_s)	2	8.40	8.97	33a′ π(C=C(CH_3)$_2$)/π(C=C)
	3	9.73	10.99	23a″ σ
4	1	7.7-8.7[e]	8.25	$27b_u$ π(C=C)/π(C=C)/π(C=C)
(C_{2h})	2	7.7-8.7	8.65	$27a_g$ π(C=C)/π(C=C)/π(C=C)
	3	7.7-8.7	9.06	$26b_u$ π(C=C)/π(C=C)/π(C=C)
	4	9.6	10.79	$18b_g$ σ
	5	10.0	11.17	$18a_u$ σ
5	1	8.11	8.55	$28a_g$ π(C=C)
(C_{2h})	2	8.11	8.58	$27b_u$ π(C=C)
	3	9.7	10.72	$18b_g$ σ

[a] E_{tot} in a.u. (see Experimental section). − [b] The assignments represent the major NBO contributions in the CMOs. − [c] Vibrational progression with peaks at 8.25 and 8.42 eV. − [d] Vibrational progression with peaks at 9.11 and 9.31 eV (Figure 4). − [e] Values derived from the calculated data by subtraction of 0.4 eV, which is the difference found between the observed and calculated positions of the central π(C=C) orbitals of **1**, **2** and **15** (see ref.[2]). In the PE spectrum of **4** a broad band is found between 7.7−8.7 eV with distinct maxima at 7.9, 8.1 and 8.3 eV (Figure 4).

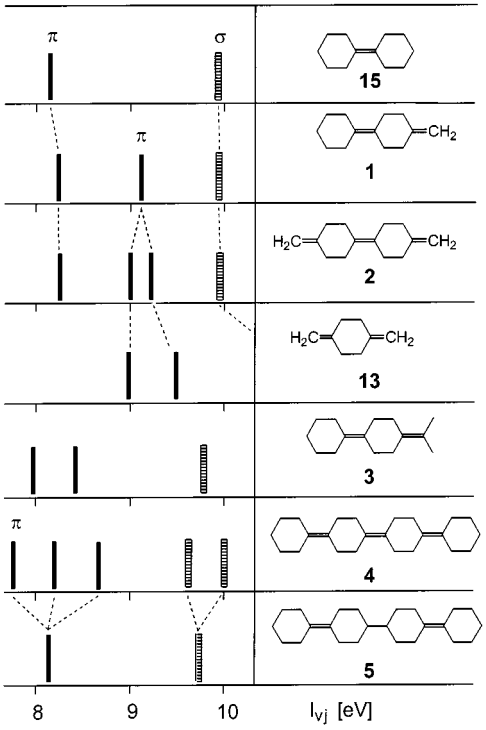

Figure 5. Correlation diagram of the first ionization energies, I_{vj}, of **1**−**5**, **13** and **15** (Figures 1 and 2).

solved bands are found at 9.4 eV, 9.80 eV and 10.2 eV. The PE spectrum of **10** shows two well resolved bands at 8.2 eV and 8.71 eV, together with three partially overlapping bands at 9.4 eV, ca. 10.0 eV and 10.4 eV. The overlap of bands is even stronger in the PE spectrum of **18**; only two bands at ca. 9.1 eV and ca. 9.8 eV are discernible. The 8.33 eV band of **9** is attributed to an ionization at the π(C=C) orbital. Correlation of the bands at higher I_{vj} values of **9**, **10** and **18** with the first two bands of cyclohexanone oxime [**19**, 9.4 eV and 9.8 eV (Figure 2)] suggests that they must be assigned to ionizations at the π(C=N−O) and the Lp_σ(N) orbitals, respectively (Figure 9 and Table 4).[30] In analogy to ketone **8**, comparison of the PES bands of **10** at 8.2 eV and 8.71 eV with those of **20** shows that these must be attributed to ionizations from the two linear combinations of the π(C=C) and Lp_π(S) orbitals.[2] The separation of these bands (ΔI_{vj} 0.51 eV) corresponds with that found for both **20** (ΔI_{vj} 0.47 eV) and **8** (ΔI_{vj} 0.57 eV). These assignments are supported by RHF/6−31G* calculations (Table 4).

A comparison of the position of the π(C=C) band of **9** (8.33 eV) or the center of gravity (8.46 eV) of the linear combination bands of **10** (8.2 eV and 8.71 eV) with that of the π(C=C) band of **15** (8.16 eV[2]) provides an estimate of the inductive effect of the C=N−O functionality (ca. 0.2 eV).

The He^I PE spectrum of **11** shows two broad bands at 8.75 and 10.4 eV, of which the latter overlaps with a band positioned at 10.1 eV. Correlation with the bands of **15** (8.16 eV) suggests that the first band of **11** (8.75 eV) must be attributed to an ionization at the π(C=C) orbital, taking into account an inductive effect of ca. 0.6 eV for the π(C=C($CN)_2$) functionality. This value was estimated from the difference between the position of the σ-orbitals of **11** (10.4 eV) and **15** (9.80 eV,[2] Figures 8 and 9 and Table 4). RHF/6−31G* calculations corroborate this assignment.

In the case of **12**, four resolved PES bands are found (Figure 8 and Table 4). Correlation with the bands found for **11** indicates that the 9.95 eV band must be assigned to an ionization from the π(C=C(CN_2)) orbital. In addition, correlation with bands found for **20** indicates that the 8.53 eV and 9.08 eV bands of **12** originate from ionizations of the two linear combinations of the π(C=C) and Lp_π(S) orbitals [cf. **20**; a′ π/Lp_π(S) 8.16 eV and a′ Lp_π(S)/π 8.63 eV].[2] The shift of both levels to higher energy is due

Table 3. Vertical ionization energies I_{vj} [eV] and RHF/6−31G* orbital energies $-\varepsilon_j$ [eV] and assignments of *anti*-**6−8**, with $-\varepsilon_j$ [eV] values for the *twist-boat* conformer (C_i) of **7** in square brackets

Compound[a]	Band (*j*)	I_{vj}	$-\varepsilon_j$	Assignment[b]
6	1	8.53	9.04	30a′ π(C=C)
(C_s)	2	9.15	10.57	19a′′ Lp_n(O)
	3	10.2	11.58	18a′′ σ
	4		12.37	29a′ σ
7	1	8.8	9.51 [9.27]	$16b_u$ π(C=C) [$26a_u$ π(C=C)]
(C_{2h})	2	9.2	10.72 [10.70]	$10b_g$ Lp_n(O)/σ [$26a_g$ Lp_n(O)/σ]
	3	9.3	10.91 [10.89]	$10a_u$ Lp_n(O)/σ [$25a_u$ Lp_n(O)/σ]
	4	10.9	12.28 [12.21]	$9b_g$ σ [$25a_g$ σ]
8	1	8.37	8.99	33a′ Lp_π(S)/π(C=C)
(C_s)	2	8.94	9.55	32a′ π(C=C)/Lp_π(S)
	3	9.2	10.72	20a′′ Lp_n(O)
	4	10.5	11.58	31a′ Lp_n(S)/σ
	5	10.8	11.91	19a′′ σ

[a] E_{tot} in a.u. (see Experimental section). − [b] The assignments represent the major NBO contributions in the CMOs.

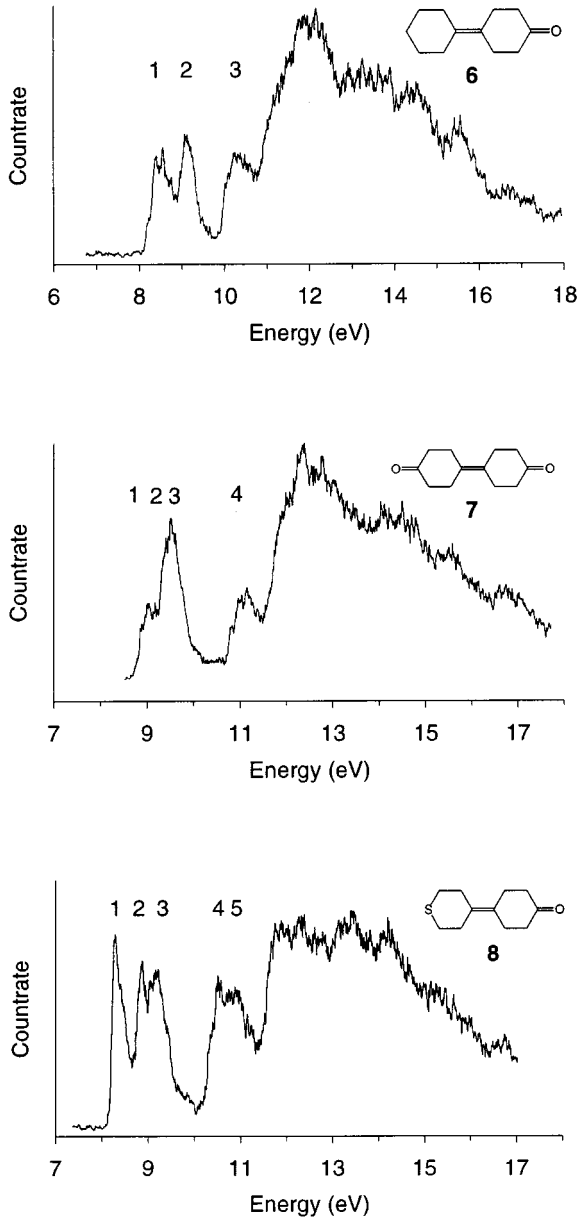

Figure 6. He^I Photoelectron spectra of **6−8**.

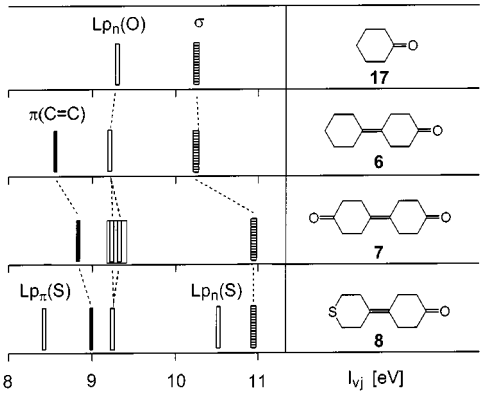

Figure 7. Correlation diagram of the first ionization energies, I_{vj}, of **6−8** and **17** (Figure 1 and 2).

to the inductive effect imposed by the $C=C(CN)_2$ functionality (Figure 9). A comparison with the calculated $-\varepsilon_j$ values also indicates that the broad band discernible at 10.8 eV in the PE spectrum of **12** is due to ionization at an orbital consisting of the σ-type lone pair on sulfur Lp_n(S) and skeletal σ-orbitals.

Analysis of σ-π Interactions in 2 and 6−12

To study in detail the interactions between the functional groups in **2** and **6−12**, RHF/6−31G*/NBO analyses were performed using the Weinhold Natural Bond Orbital (NBO) localization procedure.[11−13] This analysis consists first of transformation of the RHF/6−31G* canonical MOs (CMOs) into a set of localized NBOs. Their interactions can be evaluated in stepwise manner, permitting the construction of MO interaction diagrams that reveal the influences of TS and/or TB interactions on the self-energies of the NBOs involved in the distinct steps (see also the legends to Figure 10−13).[11−13]

In Figure 10, the MO interaction diagram of **2** is shown with the localized π(C=C) and π(C=CH_2) self-energies after through-space interaction (NBO/TS); i.e. TS interaction is negligible.[31] In the TB1 step, the π(C=C) and the π(C=CH_2) NBO interact strongly with a precanonical MO (PCMO) consisting of four $H_{ax}-C-C-H_{ax}$ NBOs of the cyclohexyl-type rings, and are both destabilized. When

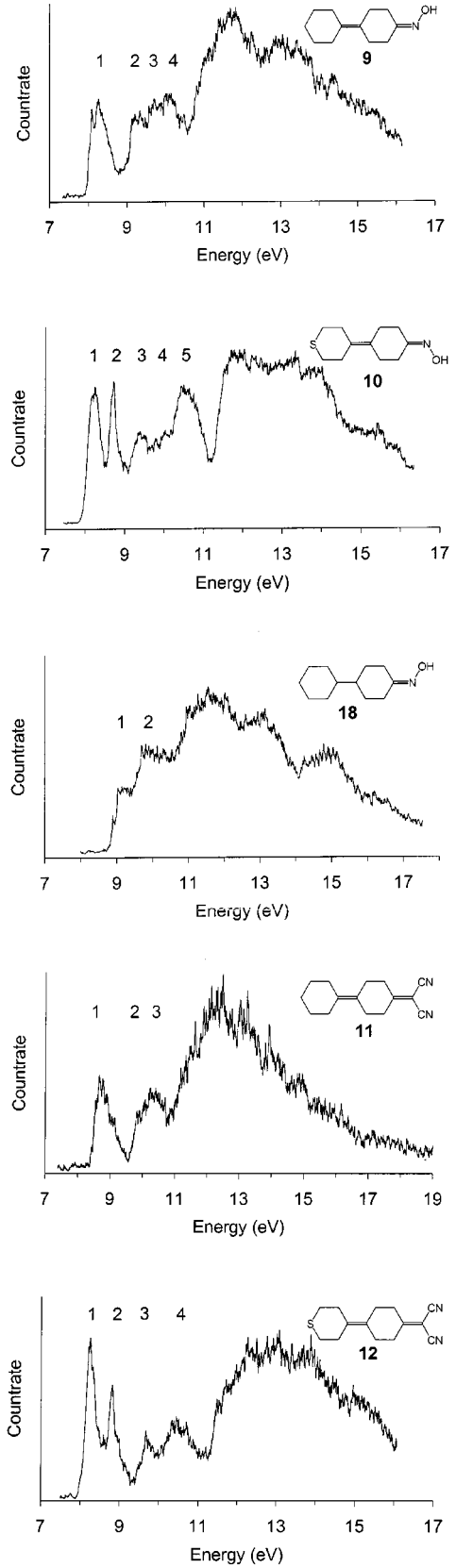

Figure 8. He[I] Photoelectron spectra of **9**–**12** and **18**.

these π-NBOs are allowed to interact simultaneously with the four $H_{ax}-C-C-H_{ax}$ NBOs (TB2), a splitting of the semi-localized π(C=CH_2) PCMOs is found, almost reproducing that of the CMOs. In the TB3 step, the levels of the semi-localized TB2 PCMOs are stabilized towards those of the CMOs when all *anti*-bonding orbitals of the interacting fragments are included. This result does not change upon admixture of other σ-orbitals. Hence, as found previously for **15** and **16**,[2] the σ-π interactions are relayed solely via these $H_{ax}-C-C-H_{ax}$ PCMOs.

NBO analyses of the ketones **6**–**8** reveal that the Lp_n(O) NBOs do not interact with the available $H_{ax}-C-C-H_{ax}$ PCMOs; this is illustrated for **7** and **8** in Figure 11. Whereas TB1 represents interaction of either of the high-lying Lp_n(O) NBOs with the $H_{ax}-C-C-H_{ax}$ PCMOs, in TB2 simultaneous interaction of the NBOs and these PCMOs is allowed. In both steps, the positions of the self-energies of the Lp_n(O) orbitals remain unaffected. In contrast, the π(C=C) NBOs of **6** (not shown), **7** and **8**, as well as the Lp_π(S) NBO of **8**, are destabilized in the TB1 step. Furthermore, the π(C=C) and Lp_π(S) PCMOs after TB1 repel each other in the TB2 step. The splitting is in agreement with that found for **20**.[2] Although, because of their symmetry mismatch, the Lp_n(O) levels cannot interact with the $H_{ax}-C-C-H_{ax}$ PCMO, the Gaussian shape of their PES bands suggests that mixing with other σ-orbitals occurs (vide supra, Figure 6). This is corroborated by the TB3 step. While the Lp_n(O) levels strongly destabilize upon interaction with two σ(C–CO) PCMOs and the nearest four $C-H_{eq}$ NBOs, the semi-localized π(C=C) PCMOs obtained after TB2 remain unaffected. Hence, the Lp_n(O)s are decoupled from the central π(C=C) NBO and other orbitals of similar symmetry. NBO analysis shows that the splitting calculated for the Lp_n(O)s of **7** ($\Delta-\varepsilon_j$ 0.19 eV, Table 2) is due to TB interactions with the $C-H_{eq}$ NBOs (TB3). Since the π(C=O) NBOs of **6**–**8** are strongly stabilized (e.g. **6**: −13.89 eV), coupling with other π-type NBOs will not occur even after interaction with the $H_{ax}-C-C-H_{ax}$ PCMOs (e.g. **6**: −12.56 eV). Thus, the π(C=O) orbital of the C=O moiety is also decoupled from the skeletal orbitals, and so the C=O moiety will only exert an inductive effect. On inclusion of all *anti*-bonding orbitals of the fragments (TB4), the semi-localized TB3 PCMO levels are stabilized toward the corresponding CMO levels; a similar observation was made in the case of **2** (TB3, Figure 10).

In the case of oxime **9**, interaction of the $H_{ax}-C-C-H_{ax}$ PCMO and terminal $C-H_{eq}$ NBO with the π(C=C) NBO or the π(C=N–O) PCMO induces a stronger destabilization of the former (TB1, Figure 12). Simultaneous interaction of the π(C=N–O) and the π(C=C) PCMO leads to a small repulsion of the levels (TB2); only a small interaction is discernible. For oxime **10**, interaction of the $H_{ax}-C-C-H_{ax}$ PCMOs with the π(C=C) or Lp_π(S) NBOs or the π(C=N–O) PCMO also results in the strongest destabilization of the π(C=C) NBO (TB1, Figure 12). Just as in the NBO analysis of **8**, the levels of the resulting TB1 π(C=C) and Lp_π(S) PCMOs become almost equal. Hence, upon simultaneous interaction of the $H_{ax}-C-C-H_{ax}$ PCMO with the π(C=C) and Lp_π(S) NBOs, as well as the π(C=N–O) PCMO, the π(C=C) and

Table 4. Vertical ionization energies I_{vj} [eV] and RHF/6−31G* orbital energies $-\varepsilon_j$ [eV] and assignments of *anti*-**9**, *anti*-**12** and *anti*-**18**

Compound[a]	Band (j)	I_{vj}	$-\varepsilon_j$	Assignment[b]
9	1	8.33	8.81	53a π(C=C)
(C_1)	2	9.4	10.10	52a π(C=N)
	3	9.80	10.99	51a Lp_σ(N)
	4	10.2	11.47	50a σ
10	1	8.2	8.83	57a Lp_π(S)/π(C=C)
(C_1)	2	8.71	9.35	56a π(C=C)/Lp_π(S)
	3	9.4	10.25	55a π(C=N)
	4	≈10.0	11.17	54a Lp_σ(N)
	5	10.4	11.46	53a Lp_n(S)/σ
11	1	8.75	9.36	36a′ π(C=C)/ π(C=C(CN)$_2$)
(C_s)	2	10.1	10.45	35a′ π(C=C(CN)$_2$)/ π(C=C)
	3	10.4	11.81	25a′′ σ
12	1	8.53	9.22	39a′ Lp_π(S)/π(C=C)
(C_s)	2	9.08	9.81	38a′ π(C=C)/Lp_π(S)/π(C=C(CN)$_2$)
	3	9.95	10.59	37a′ π(C=CCN$_2$)/π(C≡N)/π(C=C)
	4	10.8	11.80	36a′ Lp_n(S)
18	1	9.1	9.96	54a π(C=N)
(C_1)	2	9.8	10.91	53a Lp_σ(N)

[a] E_{tot} in a.u. (see Experimental section). − [b] The assignments represent the major NBO contributions in the CMOs.

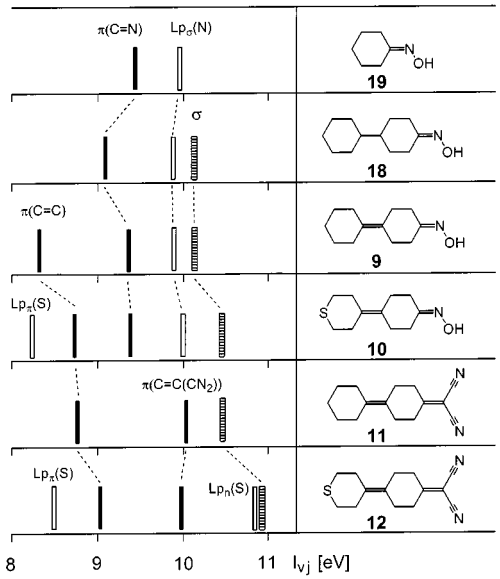

Figure 9. Correlation diagram of the first ionization energies, I_{vj}, of **9**−**12**, **18** and **19** (Figures 1 and 2).

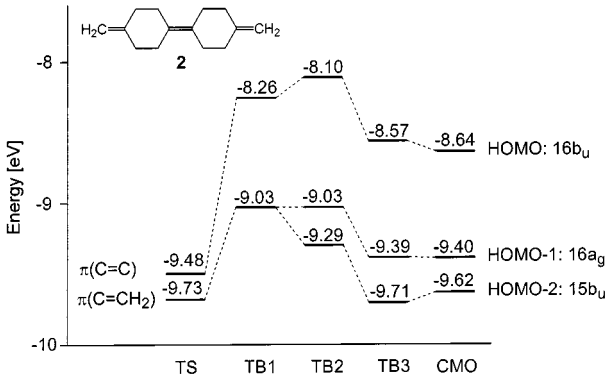

Figure 10. TS/TB interaction diagram (RHF/6−31G* NBO analysis) for **2**. TS: self-energy of the π-NBOs after TS interaction; TB1: energy of each π-NBO after interaction with the σ-orbitals ($H_{ax}-C-C-H_{ax}$ PCMOs); TB2: energy after simultaneous interaction of the π−NBOs with the $H_{ax}-C-C-H_{ax}$ PCMOs; TB3: TB2 + interaction with *anti*-bonding $H_{ax}-C-C-H_{ax}$ PCMOs; CMO: energy of the CMOs.

Lp_π(S) NBOs interact and split (TB2), as seen for **8** (vide supra) and **20**.[2] However, the π(C=N−O) level is only slightly stabilized, as in **9**. This again indicates that its interaction with either of the Lp_π(S)/π(C=C) linear combinations is very small. As observed for the Lp_n(O)s of **6**−**8**, the Lp_σ(N)s of **9** and **10** do not interact with the $H_{ax}-C-C-H_{ax}$ PCMO, but are strongly destabilized by interaction with the σ(C−CN) PCMO (TB3, Figure 12). The admixture of the σ(C−CN) PCMO may also account for the broad Lp_σ(N) bands in the PE spectra of **9** and **10** (Figure 8).[9,27]

The interaction diagrams for the dicyanomethylidene derivatives **11** and **12** again show that TS interactions between all π-like NBOs and PCMOs are negligible (TS, Figure 13).[31] TB interactions of each of the units with the eight $H_{ax}-C-C-H_{ax}$ NBOs and also, for **11**, with the terminal $C-H_{eq}$ NBOs destabilizes the π(C=C) NBOs, positioning them above the π(C=C(CN)$_2$) PCMOs, but below the Lp_π(S) level in the case of **12** (TB1 step). Upon simultaneous interaction of the π-NBOs and PCMOs with the available skeletal PCMO (TB2), the upper and lower levels repel each other. Although the PCMO sequence is now similar to that of the CMOs, the CMO energy differences are approximately twice as large. Upon admixture of the appropriate *anti*-bonding orbitals of all interacting fragments, the CMO energy differences are almost reproduced (TB3).

Conclusions

He^I PES measurements and RHF/6−31G* calculations using Koopmans' theorem in combination with RHF/6−31G*/NBO analyses of the functionalized bicyclohexylidenes **1**−**12** and functionalized bicyclohexyl derivative **18**,

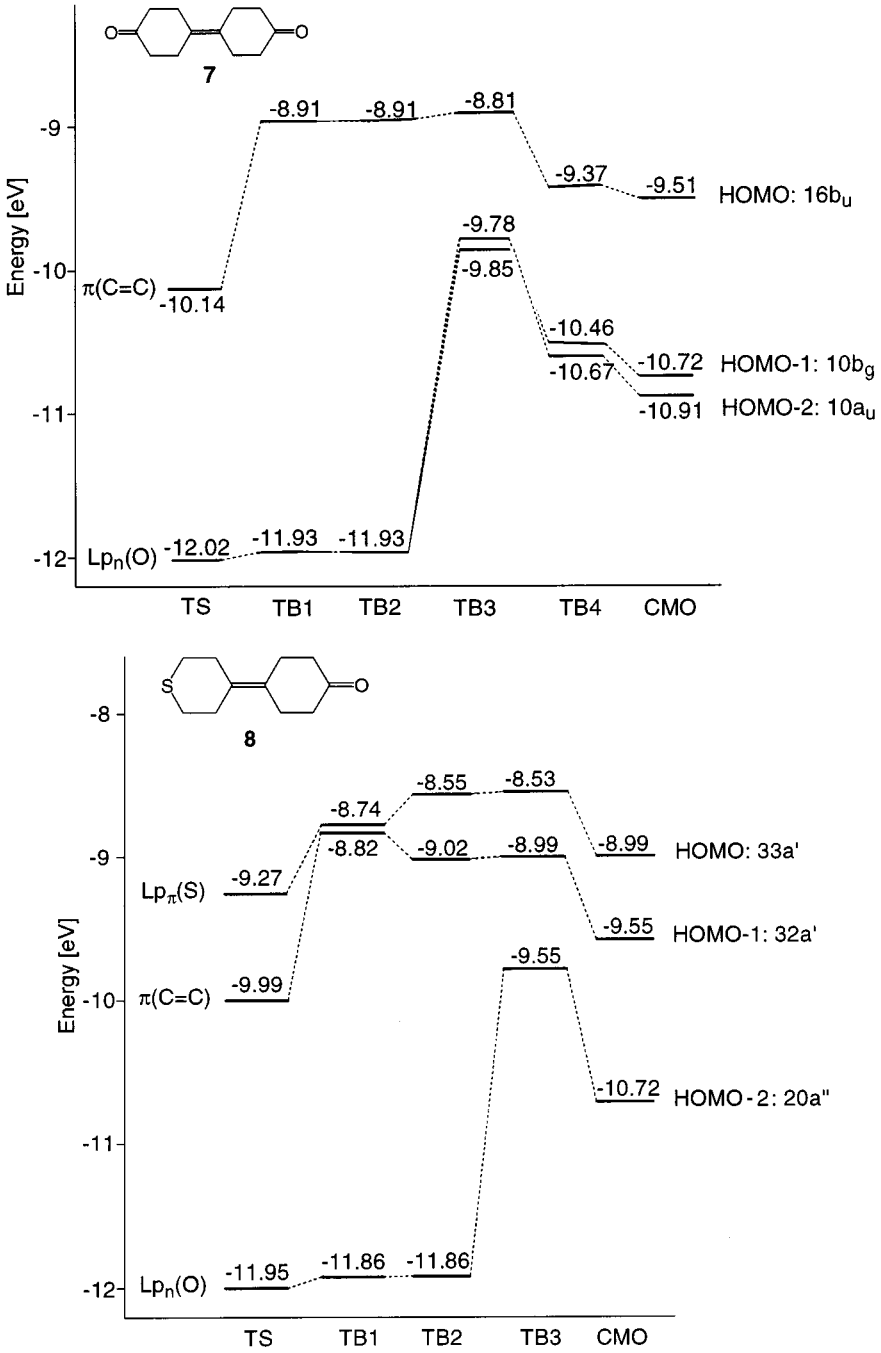

Figure 11. TS/TB interaction diagrams (RHF/6−31G* NBO analysis) of **7** and **8**. For the meaning of TS, TB1, TB2 and CMO see legend of Figure 10; TB3: TB2 + interaction with the two σ(C−CO) PCMOs and the $C-H_{eq}$ NBOs nearest to the C=O moieties. TB4: TB3 + all corresponding *anti*-bonding orbitals.

show that, in the case of **1**−**4**, **8**, **10** and **11**−**12**, ground-state TB electronic interactions occur between π-type orbitals in the functional groups and the π(C=C) orbitals. The TB interactions are relayed through the $H_{ax}-C-C-H_{ax}$ σ-orbitals of the cyclohexyl-like moieties.

Upon going from **1** to **3**, TB interaction between π(C=C) and terminal π(C=CH_2) or π(C=C(CH_3)$_2$) units increases because of the smaller energy difference between the interacting units in **3**. Whereas, in the case of **2**, the two linear combinations of the terminal π(C=CH_2) orbitals are split by ΔI_{vj} 0.30 eV ($\Delta-\varepsilon_j$ 0.22 eV), this splitting increases for structurally related **4** ($\Delta-\varepsilon_j$ 0.41 eV). This is attributed to the improved energy matching of the π-orbitals in **4**, with respect to **2**. As a consequence of the large energy separation between the π(C=O) and π(C=C) orbitals, TB interactions are absent in the cases of **6**−**8**. Similar results are found for the oximes **9** and **10**. Ketone **8** and oxime **10** notwithstanding, TB interaction between the π(C=C) and the 3p-sulfur lone pair [Lp$_\pi$(S)] orbitals has been unequivocally identified. In both cases, these interactions resemble that previously found for **20**.[2] For **11** and **12**, TB interaction is discernible between the π(C=C($CN)_2$) and π(C=C)

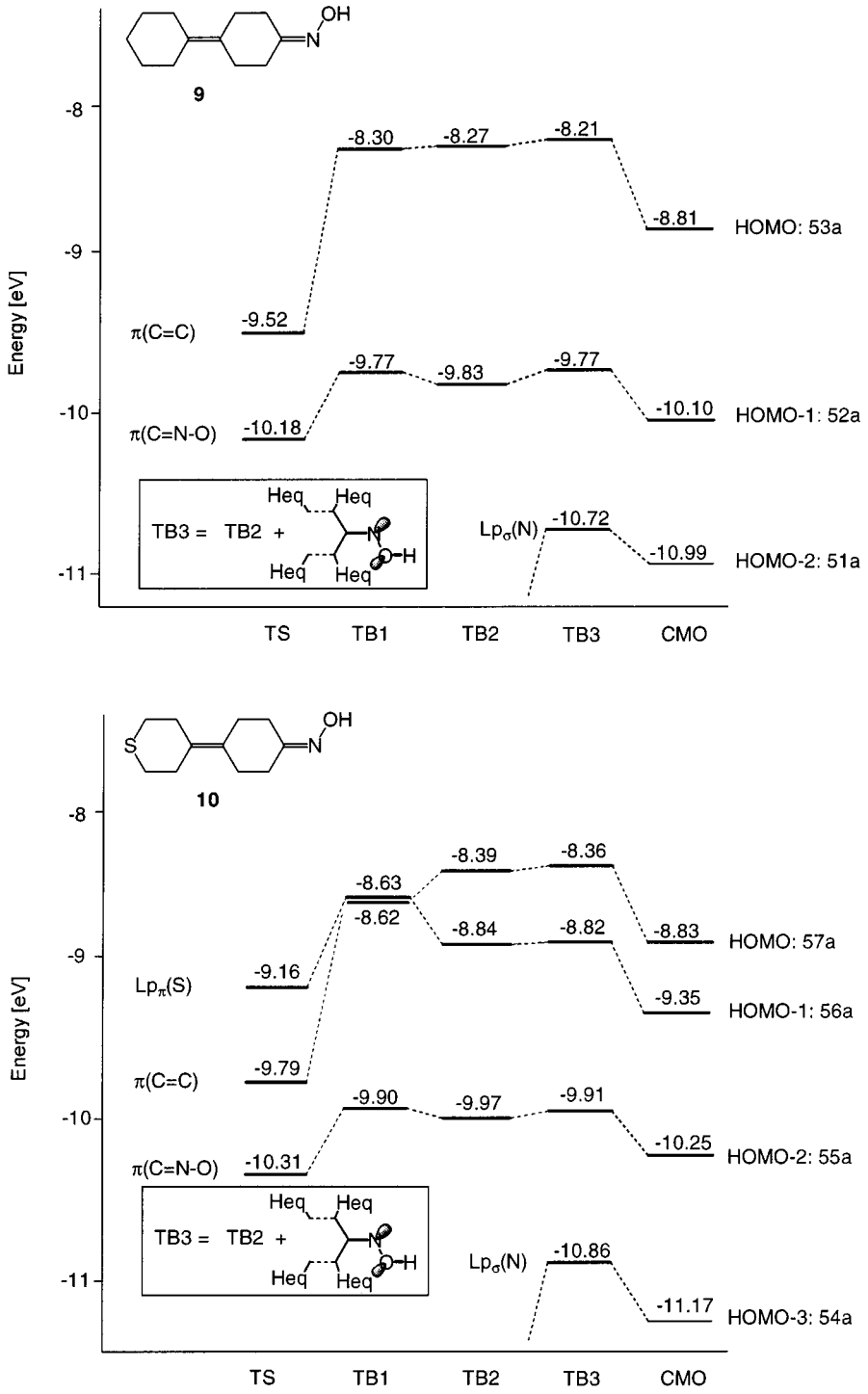

Figure 12. TS/TB interaction diagram (RHF/6−31G* NBO analysis) of **9** and **10**. For the meaning of TS, TB1, TB2 and CMO see legend of Figure 10. TB3: TB2 + additional NBOs indicated in the Figure.

orbitals, further modified in the case of **12** by coupling with the 3p-sulfur lone pair [$Lp_{\pi}(S)$].

Experimental Section

Analytical Techniques: Melting points (uncorrected) were determined using a Mettler FP5/FP51 apparatus. − NMR: spectra were recorded on a Bruker AC 300 (^1H 300.133 MHz and ^{13}C 75.47 MHz) spectrometer in $CDCl_3$ unless stated otherwise; chemical shifts are reported downfield from internal TMS. − IR measurements were performed on powder samples diluted with KBr using a Mattson FT-IR 2000 spectrometer equipped with a diffuse reflectance accessory. − Elemental analyses were performed by Dornis & Kolbe, Microanalytisches Laboratorium, Mülheim a.d. Ruhr, Germany. Dry THF and CH_2Cl_2 were prepared by distillation from Na and $CaCl_2$, respectively. DMSO was dried with 3-Å molecular sieves and deoxygenated by three consecutive freeze-thaw cycles.

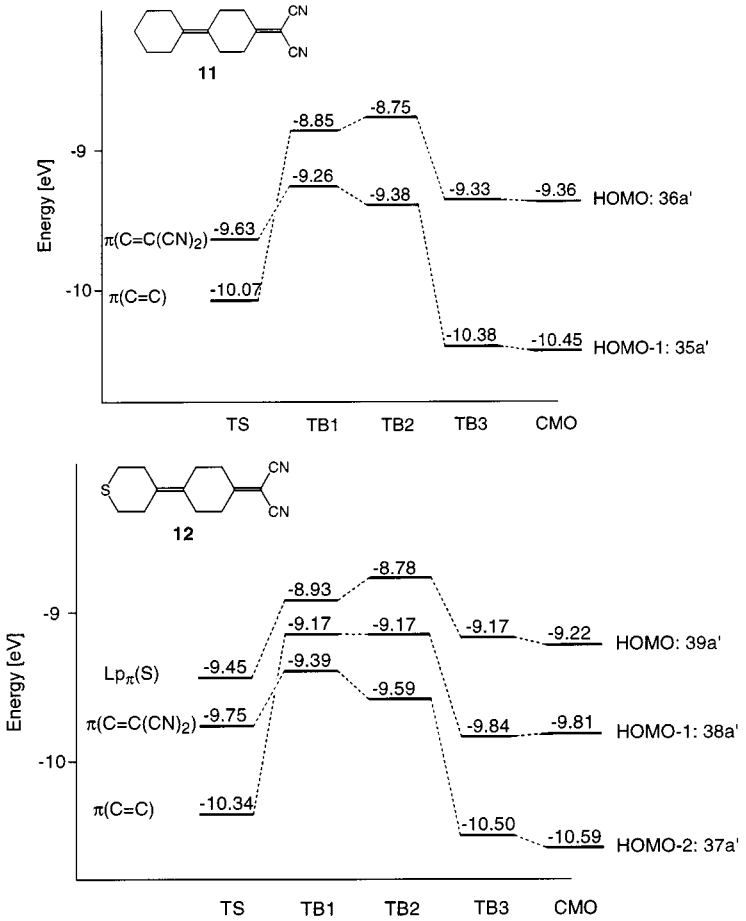

Figure 13. TS/TB interaction diagram (RHF/6−31G* NBO analysis) of **11** and **12**. For the meaning of TS, TB1, TB2 and CMO see legend of Figure 10.

4-Methylidene-1,1′-bicyclohexylidene (1): Compound **1** was prepared by addition of **6** (6.40 g, 0.04 mol) to a solution of NaH (0.86 g, 0.04 mol, washed with *n*-pentane) and triphenylmethylphosphonium bromide (98%, 12.9 g, 0.04 mol) in dry, deoxygenated DMSO. The reaction mixture was stirred at 50 °C overnight. After cooling to room temperature, the reaction was terminated by addition of H_2O (200 mL). Extraction of the reaction mixture with *n*-pentane (5 × 50 mL), followed by drying of the combined organic layers (Na_2SO_4), filtration over charcoal and removal of the solvent by evaporation in vacuo afforded crude **1** (6.12 g, 95%). A sample (2.33 g) was purified by recrystallization from hot MeOH (50 mL), followed by sublimation (0.005 Torr, 40 °C): Yield 90%; m.p. 53.9 °C. − ^{1}H NMR: δ = 1.56 (m, 6 H), 2.13−2.28 (m, 12 H), 4.64 (s, 2 H). − ^{13}C NMR: δ = 27.2, 28.7, 30.3, 30.6, 36.3, 106.9, 127.6, 131.0, 149.7. − $C_{13}H_{20}$: calcd. C 88.57, H 11.43. found C 88.36, H 11.32.

4,4′-Dimethylidene-1,1′-bicyclohexylidene (2): Following the procedure for **1**, **7**[1d] (1.0 g, 5.20 mmol) was converted into **2** using NaH (0.28 g 11.7 mmol, washed with *n*-pentane) and triphenylmethylphosphonium bromide (98%, 3.80 g, 10.6 mmol) in DMSO (25 mL). Crude **2** (0.7 g, 3.7 mmol, 71%) was obtained as described for **1** and purified by recrystallization from MeOH (10 mL, −20 °C), followed by sublimation (0.005 Torr, 80 °C): Yield 85%; m.p. 58.3 °C. − ^{1}H NMR: δ = 2.20 (m, 8 H), 2.28 (m, 8 H), 4.65 (s, 4 H). − ^{13}C NMR: δ = 30.8, 36.3, 107.1, 129.2, 149.3. − $C_{14}H_{20}$: calcd. C 89.30, H 10.70. found C 89.18, H 10.64.

4-Isopropylidene-1,1′-bicyclohexylidene (3): Compound **6** (2.50 g, 14.0 mmol) was first converted into the β-hydroxy acid, 2-(1,1′-bicyclohexlidene-4-yl)-2-hydroxypropanoic acid, by reaction with isobutyric acid (1.23 g, 14.0 mmol), using LDA (3.0 g, 29.4 mmol) in dry THF (60 mL) according to a procedure described elsewhere.[1] Overnight drying of the crude β-hydroxy acid, in a vacuum desiccator over P_2O_5, gave material sufficiently pure for further use (3.2 g, 12.0 mmol, 83%): ^{1}H NMR: (5% [D$_6$]DMSO in $CDCl_3$): δ = 1.21 (2, 6 H), 1.41−1.58 (m, 8 H), 1.69 (m, 2 H), 2.10 (m, 2 H), 2.17 (m, 4 H), 2.54 (m, 2 H). − ^{13}C NMR (5% [D$_6$]DMSO in $CDCl_3$): δ = 20.8, 24.1, 26.9, 28.3, 29.8, 33.0, 49.1, 74.0, 127.6, 129.5, 180.3.

The crude β-hydroxy acid (3.0 g, 11.3 mmol) was decarboxylated and dehydrated using *N,N*-dimethylformamide dineopentyl acetal (5.21 g, 22.6 mmol) in dry CH_3CN (125 mL) according to a literature procedure,[1a] yielding **3** (2.0 g, 9.8 mmol, 87%) as a white solid. Sublimation (0.02 Torr, 80 °C) of a sample gave pure **3**: m.p. 102.8 °C. − ^{1}H NMR: δ = 1.45−1.69 (m, 6 H), 1.66 (s, 6 H), 2.17 (m, 4 H), 2.23 (m, 8 H). − ^{13}C NMR: δ = 19.9, 27.2, 28.5, 28.9, 29.8, 30.1, 121.0, 127.8, 130.3, 131.0. − $C_{15}H_{24}$: calcd. C 88.16, H 11.84. found C 88.13, H 11.90.

4-[4-(Dicyanomethylidene)cyclohexylidene]tetrahydro-*4H*-thiopyran (12): A mixture of 4-(tetrahydro-4*H*-thiopyran-4-ylidene)cyclohexanone (**8**,[1a] 0.58 g, 2.96 mmol), malonitrile (0.21 g, 3.18 mmol), ammonium acetate (0.26, 3.34 mmol) and acetic acid (0.50 mL) in C_6H_6 was heated to reflux temperature in a Dean−Stark apparatus until the theoretical amount of H_2O had been collected (0.05 mL). The reaction mixture was subsequently cooled to room temperature, and poured into H_2O saturated with $NaHCO_3$ (50 mL), after which the layers were separated. The aqueous layer was extracted

with $CHCl_3$ (3 × 50 mL) and the combined organic fractions washed with H_2O (2 × 25 mL), dried with Na_2SO_4 and evaporated to dryness in vacuo, yielding crude **12** (0.50 g, 2.04 mmol, 69%). Recrystallization from ethyl acetate gave pure product: Yield 52%; m.p. 166 °C. – ^{1}H NMR: δ = 2.46 (m, 4 H), 2.58 (m, 4 H), 2.67 (m, 4 H), 2.75 (m, 4 H). – ^{13}C NMR: δ = 27.8, 30.4, 32.2, 34.2, 83.4 111.5, 125.4, 132.0, 184.0. – IR: $\tilde{\nu}$ = 1587 [C=C(CN)$_2$], 2231 (C≡N) cm^{-1}. – $C_{14}H_{16}N_2S$: calcd. C 68.82, H 6.60, N 11.46, S 13.12. found C 68.67, H 6.51, N 11.51.

1,1′:4′,1′′:4′′,1′′′-Quatercyclohexylidene (**4**),[1a] 4,4′-bis(cyclohexylidene-1,1′-bicyclohexyl) (**5**),[15] 1,1′-bicyclohexyliden-4-one (**6**),[1a] 1,1′-bicyclohexylidene-4,4′-dione (**7**),[1a] 4-(tetrahydro-4*H*-thiopyran-4-ylidene)cyclohexanone (**8**),[1a] 1,1′-bicyclohexyliden-4-one oxime (**9**),[1b] 4-(dicyanomethylidene)-1,1′-bicyclohexylidene (**11**)[17] and 4-cyclohexylcyclohexanone oxime (**18**)[15] were all prepared using previously reported procedures.

He^I Photoelectron Spectroscopy: The He^I PE spectra were recorded on a Perkin–Elmer PS 18 spectrometer at the following temperatures: **1**, 34 °C; **2**, 34 °C; **3**, 70 °C; **4**, 175 °C; **5**, 175 °C. **6**, 50 °C; **7**, 105 °C; **8**, 90 °C; **9**, 100 °C; **10**, 100 °C; **11**, 120 °C; and **12**, 160°C. The calibration was performed with Ar (15.76 and 15.94 eV) and Xe (12.13 and 13.44 eV). Resolution was 20 meV on the $^2P_{3/2}$ Ar line.

Ab initio Calculations: Compounds **1**–**12** and **18** were optimized at the RHF/6–31G* level of theory using GAMESS-UK.[32] The optimized geometries were characterized as genuine minima by Hessian calculations [C_s: *anti*-**1** (E_{tot} −503.911529 a.u.), *anti*-**3** (E_{tot} −581.977646 a.u.), *anti*-**6** (E_{tot} −539.762716 a.u.), *anti*-**8** (E_{tot} −898.234572 a.u.), *anti*-**11** (E_{tot} −687.378761 a.u.), *anti*-**12** (E_{tot} −1045.849979 a.u.) and C_{2h}: *anti*-**2** (E_{tot} −541.758209 a.u.), *anti*/*anti*/*anti*-**4** (E_{tot} −929.778393 a.u.), *anti*/*anti*/*anti*-**5** (E_{tot} −930.965436 a.u.), *anti*-**7**, chair-chair (E_{tot} −613.459520 a.u.), C_i: *twist-boat*-**7** (E_{tot} −613.455067 a.u.), C_1: *anti*-**9** (E_{tot} −594.725697 a.u.), *anti*-**10** (E_{tot} −953.197876 a.u.) and *anti*-**18** (E_{tot} −595.912171 a.u.)]. NBO analyses were performed using the NBO 3.0 program[33] as implemented in GAMESS-UK.[32] Pertinent data (optimized geometries) are available upon request from L. W. J.

[1] [1a] F. J. Hoogesteger, R. W. A. Havenith, J. W. Zwikker, L. W. Jenneskens, H. Kooijman, N. Veldman, A. L. Spek, *J. Org. Chem*. **1995**, *60*, 4375–4384. – [1b] F. J. Hoogesteger, J. M. Kroon, L. W. Jenneskens, E. J. R. Sudhölter, T. J. M. de Bruin, J. W. Zwikker, E. ten Grotenhuis, C. H. M. Mareé, N. Veldman, A. L. Spek, *Langmuir* **1996**, *12*, 4760–4767. – [1c] E. ten Grotenhuis, A. W. Marsman, F. J. Hoogesteger, J. C. van Miltenburg, J. P. van der Eerden, L. W. Jenneskens, W. J. J. Smeets, A. L. Spek, *J. Cryst. Growth* **1998**, *191*, 834–845 and references cited. – [1d] F. J. Hoogesteger, L. W. Jenneskens, H. Kooijman, N. Veldman, A. L. Spek, *Tetrahedron* **1996**, *52*, 1773–1784. – [1e] A. W. Marsman, E. D. Leusink, J. W. Zwikker, L. W. Jenneskens, W. J. J. Smeets, A. L. Spek, *Chem. Mater*. **1999**, *11*, 1484–1491.

[2] A. W. Marsman, R. W. A. Havenith, S. Bethke, L. W. Jenneskens, R. Gleiter, J. H. van Lenthe, M. Lutz, A.L. Spek, *J. Org. Chem.* in press.

[3] The precanonical molecular orbitals (PCMOs) of the $H_{ax}–C–C–H_{ax}$ units consist of linear combinations of natural bond orbitals (NBOs) of the $C–H_{ax}$ and $C–C$ bonds as obtained from the NBO analyses.[11–13]

[4] M. Allan, P. A. Snyder, M. B. Robin, *J. Phys. Chem.* **1985**, *89*, 4900–4903.

[5] E. Heilbronner, E. Honegger, W. Zambach, P. Schmitt, H. Günther, *Helv. Chim. Acta* **1984**, *67*, 1681–1690.

[6] R. Hoffmann, *Acc. Chem. Res.* **1971**, *4*, 1–9; R. Hoffmann, A. Imamura, W. J. Hehre, *J. Am. Chem. Soc.* **1968**, *90*, 1499–1509.

[7] R. Gleiter, W. Schäfer, *Acc. Chem. Res.* **1990**, *23*, 369–375.

[8] S. Winstein, *Spec. Publ. Chem. Soc.* **1967**, *21*, 5–45; P. M. Warner, *In Topics in Nonbenzenoid Aromatic Chemistry*; Hirokawa Publishing Co.: Tokyo, **1977**, vol. *2283*; L. A. Paquette, *Angew. Chem.* **1978**, *90*, 114–125.

[9] [9a] R. Gleiter, H. Lange, O. Borzyk, *J. Am. Chem. Soc*. **1996**, *118*, 4889–4895. – [9b] H. Lange, R. Gleiter, G. Fritzsche, *J. Am. Chem. Soc*. **1998**, *120*, 6563–6568.

[10] T. Koopmans, *Physica* **1934**, *1*, 104–113.

[11] E. Heilbronner, A. Schmelzer, *Helv. Chim. Acta* **1975**, *58*, 936–967; See also G. Bieri, F. Binger, E. Heilbronner, J. P. Maier, *Helv. Chim. Acta* **1977**, *60*, 2213–2233.

[12] A. E. Reed, R. B. Weinstock, F. Weinhold, *J. Chem. Phys.* **1985**, *83*, 735–746; A. E. Reed, F. Weinhold, *J. Chem. Phys.* **1983**, *78*, 4066–4073.

[13] A. Imamura, M. Ohsaku, *Tetrahedron* **1981**, *37*, 2191–2195.

[14] A. I. Vogel, *Vogel's Textbook of Practical Organic Chemistry*, Wiley & Sons, New York, **1989**, 498–499.

[15] F. J. Hoogesteger, D. M. Grove, L. W. Jenneskens, T. J. M. de Bruin, B. A. J. Jansen, *J. Chem. Soc., Perkin Trans. 2* **1996**, 2327–2333.

[16] A. W. Marsman, L. W. Jenneskens, B. L. A. van Poecke, A. L. Spek, E. T. G. Lutz, J. H. van der Maas, *Chem. Mater.* **2000,** submitted.

[17] F. J. Hoogesteger, *Ph.D. Thesis, Oligo(cyclohexylidenes). Development of Novel Functional and Organized Materials*, Utrecht University, Utrecht, The Netherlands, **1996**.

[18] N. Veldman, A. L. Spek, F. J. Hoogesteger, J. W. Zwikker, L. W. Jenneskens, *Acta Cryst*. **1994**, *C50*, 742–744.

[19] This is confirmed by the striking resemblance of the PE spectra of 1,1′-bicyclohexylidene (**15**) and those of the conformationally stable *anti*- and *syn*-conformers of 4,4′-di-*tert*-butyl-1,1′-bicyclohexylidene (*anti* ΔI_{vj} 0.12 eV and *syn* ΔI_{vj} 0.09 eV), respectively.[2]

[20] M. St-Jacques, M. Bernard, *Can. J. Chem.* **1969**, *47*, 2911–2913 and references cited.

[21] R. W. A. Havenith, J. H. van Lenthe, L. W. Jenneskens, F. J. Hoogesteger, *Chem. Phys.* **1997**, *225*, 139–152.

[22] Suitable single crystals for X-ray analysis of 1,1′:4′,1′′-tercyclohexylidene (**16**) were hitherto inaccessible. The single-crystal X-ray structure of *trans*-4,4′′-diheptyl-1,1′:4′,1′′-tercyclohexylidene has been determined.[1a,21]

[23] Similar vibrational progressions were found for ionization from orbitals involving the π(C=C) bands of **15** ($\tilde{\nu} \approx 1350$ cm^{-1}) [3] and 4-methylidene-*4H*-tetrahydropyran ($\tilde{\nu} \approx 1450$ cm^{-1}), see ref. [24]

[24] R. Sarneel, C. W. Worrell, P. Pasman, J. W. Verhoeven, G. F. Mes, *Tetrahedron* **1980**, *36*, 3241–3248.

[25] The linkage of two molecules of **15** (I_{vj} 8.16 eV) by a carbon–carbon single bond, giving **5** (I_{vj} 8.11 eV), appears to induce a small destabilization of the π(C=C) band (ΔI_{vj} 0.05 eV). This destabilization is approximately half of that found for the π(C=C) band of *anti*-4,4′-di-*tert*-butyl-1,1′-bicyclohexylidene (I_{vj} 8.04 eV) and *syn*-4,4′-di-*tert*-butyl-1,1′-bicyclohexylidene (I_{vj} 8.07 eV), see ref. [2]

[26] G. Spanka, G. Rademacher, *J. Org. Chem*. **1986**, *51*, 592–596.

[27] D. Dougherty, P. Brint, S. P. McGlynn, *J. Am. Chem. Soc*. **1978**, *100*, 5597–5603.

[28] D. O. Cowan, R. Gleiter, J. A. Hashmall, E. Heilbronner, V. Hornung, *Angew. Chem*. **1971**, *83*, 405–406.

[29] N. J., Turro, *Modern Molecular Photochemistry*, Benjamin, California **1978**, 35.

[30] A. Strenge, P. Rademacher, *Eur. J. Org. Chem.* **1999**, 1601–1609. Unfortunately, no I_{vj} values for ionizations from σ-MOs of **19** were reported in this paper.

[31] M. N. Paddon-Row, S. S. Wong, K. D. Jordan, *J. Chem. Soc., Perkin Trans. 2* **1990**, 425–430.

[32] GAMESS-UK is a package of ab initio programs written by: M. F. Guest, J. H. van Lenthe, J. Kendrick, K. Schoffel, P. Sherwood and R. J. Harrison **1998** with contributions from: R. D. Amos, R. J. Buenker, M. Dupuis, N. C. Handy, I. H. Hiller,

P. J. Knowles, V. Bonacic-Koutecky, W. Niessen, V. R. Saunders and A. J. Stone, The package is derived from the original GAMESS code due to: M. Dupuis,. D. Spangler, and J. Wendolowski, NRCC Software Catalog, Vol 1, Program No. QG01 (GAMESS) **1980**.

[33] NBO 3.0 program: *Natural Bond Orbital*/*Natural Population Analysis*/*Natural Localized Molecular Orbitals Program*, E. D. Glendering, A. E. Reed, J. E. Carpenter, F. Weinhold.

Received February 14, 2000
[O00072]